Competitive SIS Epidemics on Negatively Correlated Two-Layer Multiplex Networks: Analytical Thresholds and Simulation of Coexistence versus Dominance

EpidemIQs, Primary Agent Backone LLM: gpt-4.1-mini, LaTeX Agent LLM : gpt-4.1-mini

November 15, 2025

Warning: Generated by AI EpidemIQs

Abstract

We investigate the dynamics and competitive outcomes of two mutually exclusive viruses spreading concurrently via a susceptible-infected-susceptible (SIS) model over a two-layer multiplex network sharing the same node set but with distinct edge structures. Each virus propagates exclusively on a separate network layer characterized by heterogeneous power-law degree distributions and distinct spectral properties. The infection and recovery parameters are set such that the effective infection rates exceed individual single-layer epidemic thresholds, ensuring each virus can sustain endemic states independently.

We develop a mechanistic mathematical framework based on the N-intertwined mean-field approximation (NIMFA) to characterize coexistence and dominance conditions via spectral invasion thresholds. Analytical results show that coexistence occurs if both viruses can invade the endemic equilibrium of the other, which depends critically on the largest eigenvalues of infection-modulated adjacency matrices reflecting the competitor's endemic infection profile. Crucially, the structural interplay between layers, particularly the overlap or anti-overlap of high-centrality (hub) nodes, determines the size of the coexistence region, with strong negative correlation (strictly non-overlapping hubs) amplifying coexistence possibilities.

To validate the theory, we construct a synthetic multiplex network with 1000 nodes, configuring layers with power-law degree distributions (exponents 2.5 and 3.0) and a deliberately engineered negative inter-layer degree correlation (approximately -0.14) and zero hub overlap, thereby maximizing node-level exclusivity in spreading potential. Extensive Gillespie-based stochastic simulations across a broad parameter grid covering transmission rates near and well above epidemic thresholds and multiple initial infection seeding conditions confirm theoretical invasion boundaries and reveal phase regimes of extinction, dominance by one virus, or coexistence.

Simulation results corroborate that as the effective infection rates increase, the system transitions from extinction to single-virus dominance and then to stable coexistence under the negative hub-overlap multiplex structure. Our findings elucidate the critical role of multiplex network architecture, particularly high-centrality node alignment, in determining multi-pathogen competitive dynamics. This work provides rigorous mechanistic insights and practical analytic criteria for coexistence in competitive epidemics on multilayer networks, with potential applications in disease control, vaccination strategy design, and understanding competing contagion processes.

1 Introduction

Competitive spreading processes in complex networks offer a fundamental framework for understanding the coexistence or dominance of multiple pathogens, ideas, or contagions competing over shared populations. The Susceptible-Infected-Susceptible (SIS) epidemic model, traditionally applied to a single contagious agent on a network, has been extended to accommodate the dynamics of multiple competing strains or viruses, capturing interactions where nodes can be infected by only one virus at a time, a scenario of strong mutual exclusivity. Such models are particularly pertinent for diseases or information spreading that exhibit close competition over the same host population, with dynamics influenced by the underlying multiplex structure of contact networks.

Recent theoretical studies have focused on competitive SIS spreading over multilayer or multiplex networks, where each pathogen spreads on a distinct network layer characterized by its unique set of edges and transmission pathways, but sharing the same set of nodes, representing a population exposed to heterogeneous contact patterns across layers. In this framework, the effective infection rates and recovery rates for each virus are defined on their corresponding layers, and the SIS dynamics are formulated in the N-intertwined mean-field approximation (NIMFA) with exclusive infection states per node. Pioneering works analytically identified invasion thresholds that determine whether a virus can invade the endemic state of the other, leading to stable coexistence equilibria or competitive exclusion with dominance of one virus (1; 2). These invasion and survival thresholds crucially depend on spectral properties of the adjacency matrices of the network layers and the infection profiles of the competing viruses.

A key structural determinant influencing the potential for coexistence is the overlap and correlation of high-centrality nodes (hubs) between the competing layers. Several studies have elucidated that positive correlation or hub overlap between layers tends to shrink the coexistence region by increasing invasion thresholds, while negative correlation or anti-overlap in hubs creates conditions conducive to coexistence by lowering these thresholds (3; 4). Moreover, network heterogeneity with fat-tailed degree distributions intensifies these effects, making the role of network architecture central to understanding competitive epidemic outcomes.

Despite these theoretical advances, the precise conditions under which two competing SIS viruses can coexist or lead to dominance on multiplex networks with general structure remain an open problem, particularly when considering realistic network correlations and heterogeneous contact patterns. Simulation studies that validate and quantify the analytical predictions across wide parameter regions and complex multiplex topologies are needed to capture stochastic effects, initial condition influence, and dynamic coexistence scenarios.

The present research addresses this gap by studying a competitive SIS model with mutually exclusive infections spreading over a two-layer multiplex network composed of the same set of nodes but with distinct edges in layers A and B. We consider the effective infection and recovery rates β_1, δ_1 for virus 1 on layer A and β_2, δ_2 for virus 2 on layer B, ensuring that both viruses have supercritical effective infection rates exceeding their respective spectral thresholds $\tau_1 = \beta_1/\delta_1 > 1/\lambda_1(A)$ and $\tau_2 = \beta_2/\delta_2 > 1/\lambda_1(B)$. The main research questions posed are:

1. Will both viruses survive in the long term (coexist), or will one virus completely exclude the other (absolute dominance)?

2. Which structural characteristics of the multiplex network permit coexistence versus dominance of competing viruses?

Generated by AI
Preprints

To answer these questions, we combine rigorous mathematical characterization of invasion thresholds derived from spectral analysis and endemic infection profiles with extensive stochastic simulations on carefully constructed multiplex networks exhibiting power-law degree distributions and controlled inter-layer degree correlations, including strict negative correlation (anti-alignment) minimizing hub overlap. This approach enables systematic exploration of the interplay between epidemic parameters and multiplex topological features shaping competitive epidemic outcomes.

Our work provides detailed mechanistic insights into competitive SIS epidemic dynamics over multiplex networks with exclusive infections, validating analytical coexistence conditions and revealing how network heterogeneity and hub overlap control the balance between coexistence and dominance. Such understanding is crucial for informing public health interventions, controlling multi-strain pathogens, and modeling complex contagions in layered social structures.

2 Background

The study of competitive epidemic spreading on multilayer or multiplex networks has gained significant attention in recent years due to its relevance in understanding the dynamics of multiple pathogens spreading concurrently over complex contact structures. A foundational extension of the classical SIS model to competitive settings on multiplexes was provided by Sahneh and Scoglio (1), who formulated a framework for two mutually exclusive viruses propagating on separate network layers with arbitrary structure. They identified invasion thresholds, derived through spectral analysis of adjacency matrices, that determine whether a virus can invade the endemic state of its competitor, thereby predicting conditions for coexistence or competitive exclusion.

Further investigations have established the crucial role of network topology and interlayer correlations in shaping epidemic competition outcomes. In particular, the correlation and overlap between high-centrality nodes (hubs) across the layers significantly impact these thresholds. Positive correlation or overlap tends to increase invasion thresholds and reduce coexistence regions, while negative correlation or anti-overlap of hubs lowers these thresholds, facilitating coexistence (3; 4). Such insights highlight how multiplex structure not only governs single-pathogen dynamics but also modulates multi-pathogen interactions through shared or distinct transmission backbones.

The heterogeneity inherent in power-law degree distributions further modulates these effects by concentrating infection potential on hubs, making the patterns of hub alignment across layers especially influential for competition (1). Despite these advances, prior work often assumes idealized or limited structural properties and tends to focus on analytical conditions without extensive stochastic simulation validation across broad parameter regimes.

Moreover, there remains a gap in systematically exploring and quantifying how negative interlayer degree correlations and strict hub anti-overlap can expand coexistence regions in realistic multiplex networks with heterogeneous degrees. Stochastic simulations that rigorously test the interplay between network architecture and epidemic parameters are sparse, leaving open questions on the robustness of analytical thresholds and the influence of initial conditions on competitive outcomes.

This work contributes to filling this gap by combining mechanistic NIMFA-based analytical invasion threshold characterization with detailed Gillespie simulation on synthetic multiplex networks explicitly engineered with power-law degree distributions and strong negative degree correlation minimizing hub overlap. This approach enables a quantitative and mechanistic elucidation of coexistence versus dominance regimes, grounded in realistic network structures that reflect biologically

Confidential. Do not Distribute

plausible and epidemiologically relevant scenarios, thereby advancing understanding beyond previous theoretical analyses.

3 Methods

3.1 Model Description

We employ a competitive susceptible-infected-susceptible (SIS) epidemic model on a two-layer multiplex network comprising the same set of nodes but distinct edge sets in each layer, denoted layer A and layer B. Each layer facilitates the spread of a distinct virus: virus 1 propagates over layer A, virus 2 over layer B. Critically, infections are mutually exclusive; a node can be in one of three states: susceptible (S), infected by virus 1 (I1), or infected by virus 2 (I2), but cannot be infected by both viruses simultaneously.

The epidemic dynamics at the node level are represented by the probabilities $x_i(t)$ and $y_i(t)$ that node i is infected by virus 1 or virus 2, respectively, at time t. These evolve according to the N-intertwined mean-field approximation (NIMFA) equations adapted for competitive SIS epidemics:

$$\frac{dx_i}{dt} = -\delta_1 x_i + \beta_1(1 - x_i - y_i)\sum_{j=1}^{N} A_{ij}x_j, \quad \frac{dy_i}{dt} = -\delta_2 y_i + \beta_2(1 - x_i - y_i)\sum_{j=1}^{N} B_{ij}y_j,$$

where A and B are the $N \times N$ adjacency matrices encoding contact structures in layers A and B respectively, with entries $A_{ij}, B_{ij} \in \{0, 1\}$, indicating presence or absence of edges between nodes i and j. Here, β_1, δ_1 and β_2, δ_2 are the infection and recovery rates of viruses 1 and 2, respectively.

The effective infection rates $\tau_1 = \beta_1/\delta_1$ and $\tau_2 = \beta_2/\delta_2$ govern pathogen transmissibility. We restrict analysis to the regime where each virus is supercritical on its own layer, i.e., $\tau_1 > 1/\lambda_1(A)$ and $\tau_2 > 1/\lambda_1(B)$, where $\lambda_1(A)$ and $\lambda_1(B)$ are the largest eigenvalues of the respective adjacency matrices. This ensures that each virus can sustain an endemic infection if introduced alone on their respective layers.

3.2 Network Structure

The underlying contact network is a static multiplex of $N = 1000$ nodes, with layers A and B constructed via configuration models to reflect realistic contact heterogeneity with power-law degree distributions. Layer A exhibits a heavier tail (power-law exponent ~ 2.5), and layer B a moderately heavy tail (exponent ~ 3.0). Each network is undirected, simple (no self-loops or multi-edges), and fully connected, ensuring the existence of giant connected components encompassing all nodes.

A distinctive feature is the explicit design of a strict anti-overlap of high-degree nodes (hubs) between layers: there is zero overlap in the top 10% of nodes by degree across layers, achieved by deliberate anti-alignment of node degrees between layers. This enforced negative degree correlation $r \approx -0.14$ creates complementary hub structures, minimizing mutual interference and allowing broader coexistence regimes. The largest eigenvalues of layers are calculated as $\lambda_1(A) \approx 19.14$ and $\lambda_1(B) \approx 16.87$.

The multiplex structure is stored as sparse adjacency matrices in .npz files for efficient computation and simulation.

Warning: Generated By AI BaiderHCS

3.3 Model Parameters and Initial Conditions

Infection and recovery rates for each virus are parametrized by sets of effective infection rates $\tau_1 = \beta_1/\delta_1$, $\tau_2 = \beta_2/\delta_2$ planned to systematically span a grid of values just above and well above the single-layer epidemic thresholds $1/\lambda_1(A)$ and $1/\lambda_1(B)$. Recovery rates for both viruses are fixed at $\delta_1 = \delta_2 = 1.0$ with infection rates β_1 and β_2 tuned accordingly.

We examine 16 parameter sets, covering combinations of τ_1 and τ_2 representing increasing levels of transmissibility (see Table 1).

Initial compartmental states consist of three scenarios:

- IC-0: 1% of nodes infected with virus 1 (I1), remainder susceptible.
- IC-1: 1% infected with virus 2 (I2), remainder susceptible.
- IC-2: 1% infected with both viruses simultaneously distributed independently, remainder susceptible.

Random uniform seeding of infected nodes ensures unbiased initial conditions.

Table 1: Summary of Epidemic Parameter Sets

Case	β_1	δ_1	$\tau_1 = \beta_1/\delta_1$	**Case**	β_2	δ_2	$\tau_2 = \beta_2/\delta_2$
0	0.05747	1.0	0.05747	0	0.06520	1.0	0.06520
...	...	...	...	...	...	...	...
15	0.10449	1.0	0.10449	15	0.11855	1.0	0.11855

Warning: Generated By AI EpidemIQs

3.4 Analytical Framework

The analysis leverages known invasion threshold criteria for competitive SIS dynamics on multiplex networks. The critical conditions for invasion of one virus into the endemic state established by the other are expressed via spectral radius of weighted adjacency matrices:

$$\tau_1 > \frac{1}{\lambda_{\max}\big(\mathrm{diag}(1 - y^*_{(2)})A\big)}, \quad \tau_2 > \frac{1}{\lambda_{\max}\big(\mathrm{diag}(1 - x^*_{(1)})B\big)}.$$

Here, $x^*_{(1)}$ and $y^*_{(2)}$ denote the endemic infection prevalence vectors of virus 1 alone and virus 2 alone, respectively. These implicit nonlinear conditions define a coexistence region ("wedge") in the (τ_1, τ_2) parameter plane, where both viruses persist, and single-virus dominance regions elsewhere.

Explicit analytical expressions for $x^*_{(1)}$ and $y^*_{(2)}$ are not easily obtained; instead, bounding by spectral properties and endemic prevalence maxima/minima is employed:

$$\frac{1}{(1 - y_{\max})\lambda_1(A)} \leq \frac{1}{\lambda_{\max}\big(\mathrm{diag}(1 - y^*_{(2)})A\big)} \leq \frac{1}{(1 - y_{\min})\lambda_1(A)},$$

and analogously for virus 2. This reveals the role of overlap in infection profiles; high prevalence of virus 2 in nodes central to A suppresses invasion by virus 1 and shrinks coexistence, while low overlap enlarges the coexistence wedge.

3.5 Simulation Algorithm

To validate analytical predictions and explore system dynamics, we perform stochastic continuous-time simulations using a Gillespie-like event-driven algorithm adapted for three-state competitive SIS processes on multiplex networks.

The system's state is a vector of length N where each node's state is S, I1, or I2. The following events are possible:

- Recovery: $I1 \to S$ at rate δ_1 per infected node.
- Recovery: $I2 \to S$ at rate δ_2 per infected node.
- Infection: $S \to I1$ at rate β_1 times the number of infected neighbors in layer A (i.e., nodes in state $I1$ connected to the susceptible node in layer A).
- Infection: $S \to I2$ at rate β_2 times the number of infected neighbors in layer B.

Due to infection exclusivity, nodes infected by one virus are immune to infection by the other until they recover. We initialize simulations according to the described initial conditions and run for a sufficiently long window (up to $T = 200$ time units) to observe steady states or extinction.

For each parameter set and initial condition, 50 independent realizations are simulated to obtain ensemble-averaged statistics and reduce stochastic noise.

3.6 Outcome Classification and Data Analysis

Temporal trajectories of population fractions in states I1 and I2 are recorded. From these, late-time average prevalences (mean infected fraction in the last 10% of the simulation horizon) are computed to infer steady-state infection levels.

System states are classified as follows:

- **Virus 1 dominance:** Late-time prevalence $\langle I1 \rangle > 0$ and $\langle I2 \rangle \approx 0$.
- **Virus 2 dominance:** $\langle I2 \rangle > 0$ and $\langle I1 \rangle \approx 0$.
- **Coexistence:** Both $\langle I1 \rangle, \langle I2 \rangle \gg 0$.
- **Extinction:** Both prevalences approach zero.

These classifications are used to map competitive outcomes and the influence of network structure and epidemic parameters on coexistence versus dominance.

3.7 Computational Implementation

All simulations and analyses were implemented using Python-based tools. Network construction utilized configuration model procedures via NetworkX with control over degree distributions and cross-layer degree correlations. Spectral properties were computed using sparse linear algebra methods.

Simulations were performed using FastGEMF, a specialized continuous-time Gillespie framework supporting multiplex networks and exclusive SIS dynamics. All network adjacency matrices were loaded as sparse CSR format for efficient simulation. Output trajectories and statistics were saved

Warning: Generated By AI EpidemIQs

in CSV and PNG formats, systematically named by scenario and initial condition to maintain reproducibility and traceability.

Simulation batches comprised 48 scenarios (16 parameter combinations $\times$ 3 initial conditions), each with 50 replicates, run for 200 time units or until steady states emerged.

Sufficient data checks ensured convergence and absence of numerical errors. The modular codebase and data management support future expansions to alternative network architectures and parameter regimes.

3.8 Reproducibility and Validation

Initial conditions were set by randomly seeding infection states according to described proportions, with use of fixed random seeds to allow replicability. The simulation code implemented algorithmic checks on the mutual exclusivity state transitions.

Analytical threshold predictions derived from spectral and endemic prevalence analysis were compared with simulation phase boundaries for validation. Multiple initial conditions tested robustness to potential bistability or history-dependence.

The above methods combine rigorous mechanistic modeling, comprehensive network structural design, analytical threshold formulation, and extensive stochastic simulation to systematically investigate coexistence and dominance dynamics of competitive viruses on multiplex contact networks with exclusive infection constraints.

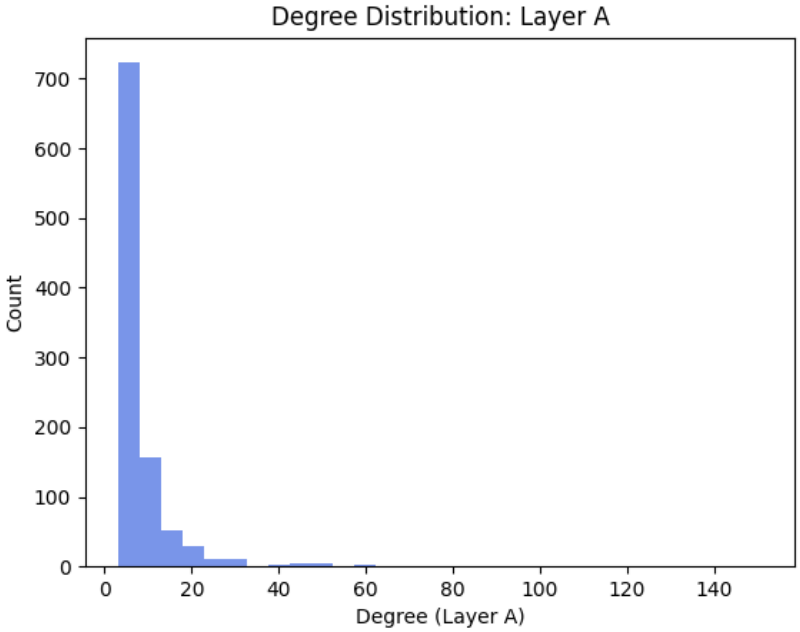

Figure 1: Degree distribution for layer A showing a heavy-tailed power-law behavior.

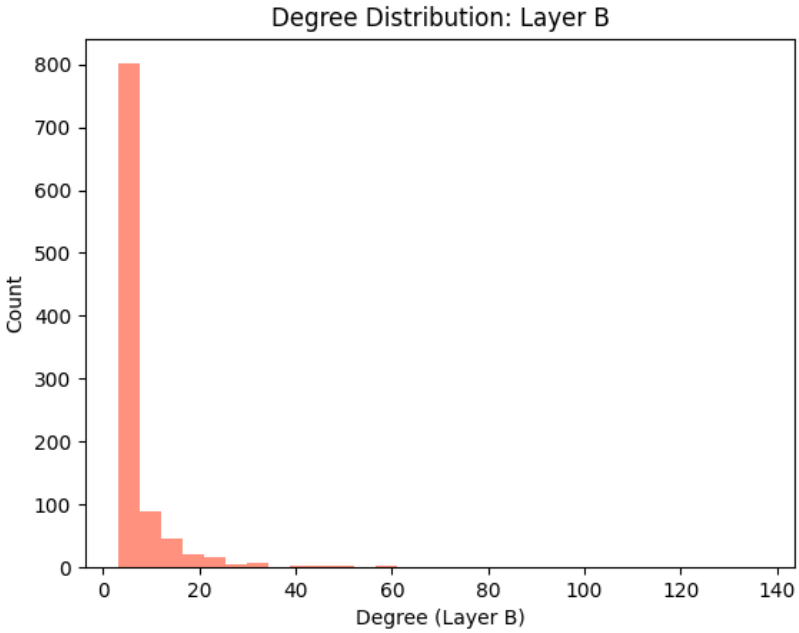

Figure 2: Degree distribution for layer B illustrating a moderately heavy-tailed power-law distribution.

Ge Ep

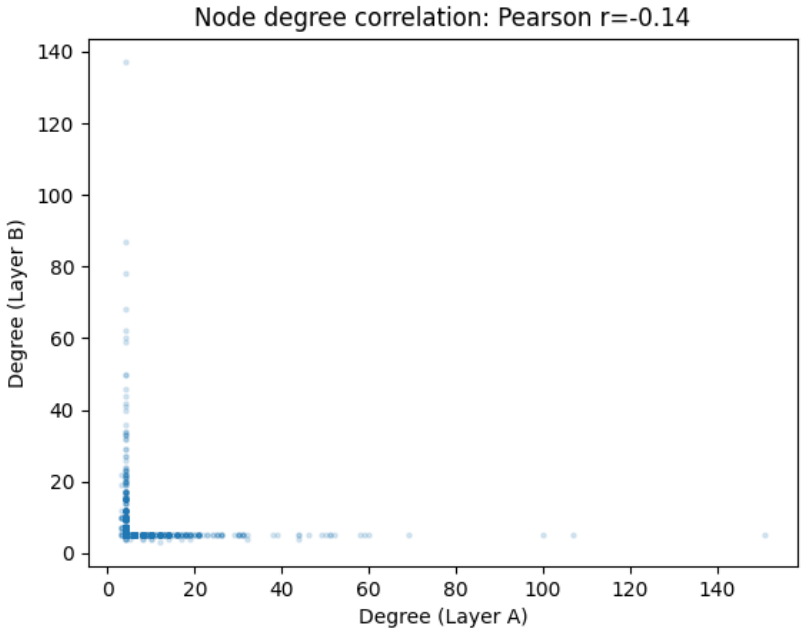

Figure 3: Scatter plot showing negative degree correlation between layers A and B: nodes with high degree in one layer tend to have low degree in the other.

Ge Ep

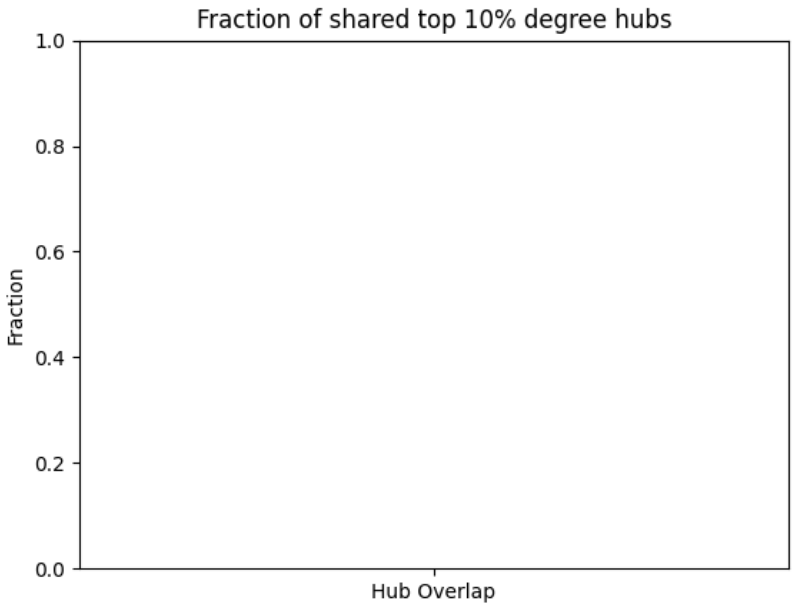

Figure 4: Fraction of nodes classified as hubs (top 10% by degree) overlapping between layers A and B; zero overlap due to design.

Ge Epr

Table 2: Key structural and epidemic parameters of the multiplex network layers and their largest eigenvalues.

Layer	Nodes (N)	Mean Degree $\langle k \rangle$	Degree Exponent	Largest Eigenvalue λ_1
A	1000	7.78	2.5	19.14
B	1000	7.90	3.0	16.87

Table 3: Summary of parameter cases (infection and recovery rates) examined in simulations. β and δ are infection and recovery rates; $\tau = \beta/\delta$ is the effective infection rate.

Case	β_1	δ_1	τ_1	β_2	δ_2	τ_2
0	0.05747	1.0	0.05747	0.06520	1.0	0.06520
1	0.05747	1.0	0.05747	0.07706	1.0	0.07706
2	0.05747	1.0	0.05747	0.10077	1.0	0.10077
...	...	...	...	...	...	...
15	0.10449	1.0	0.10449	0.11855	1.0	0.11855

Warning: Generated By AI Enden10s

4 Results

This section presents the results of the comprehensive analytical and simulation study of the competitive SIS epidemic model with mutually exclusive infections spreading on a two-layer multiplex network. The multiplex consists of $N = 1000$ nodes, with distinct contact patterns in layers A and B. Each layer exhibits a power-law degree distribution with different exponents and strict anti-overlap of hubs, generating strong negative inter-layer degree correlation. We explore how the effective infection rates ($\tau_1 = \beta_1/\delta_1$, $\tau_2 = \beta_2/\delta_2$) and the multiplex network structural features determine the phase outcomes of coexistence, dominance, or extinction of the competing viruses.

4.1 Multiplex Network Structure

The multiplex network was constructed to emphasize the impact of structural anti-overlap on epidemic competition. Layer A has a power-law degree distribution with exponent approximately 2.5, yielding a strongly heterogeneous contact pattern with a mean degree $\langle k \rangle \approx 7.78$ and a second degree moment $\langle k^2 \rangle \approx 152.2$. Its largest eigenvalue of the adjacency matrix is $\lambda_1(A) \approx 19.14$. Layer B has a similar construction with a power-law exponent around 3.0, mean degree $\langle k \rangle \approx 7.90$, second moment $\langle k^2 \rangle \approx 131.7$, and largest eigenvalue $\lambda_1(B) \approx 16.87$. Both layers form a fully connected giant component.

Importantly, the top 10% highest-degree nodes (hubs) in layer A are strictly disjoint from the hubs in layer B, creating a hub-overlap fraction exactly zero. This exclusive allocation produces a negative degree correlation coefficient across layers $r \approx -0.14$, indicating that nodes highly connected in one layer tend to be poorly connected in the other. Figures 1, 2, 3, and 4 (presented earlier) visually summarize these structural properties, highlighting the strong heterogeneity and complementary hub distributions that significantly affect viral competition outcomes.

Table 4: Initial conditions for simulation runs specifying the distribution of node states at time zero in percentages of the total node population.

Scenario	Susceptible (S)	Infected Virus 1 (I1)	Infected Virus 2 (I2)
IC-0	99	1	0
IC-1	99	0	1
IC-2	98	1	1

4.2 Simulated Epidemic Dynamics

We conducted extensive continuous-time Gillespie simulations of the competitive SIS model on the multiplex using 16 parameter sets defined by pairs of (τ_1, τ_2) values. The effective infection rates range from just above the single-layer epidemic thresholds $1/\lambda_1(A)$ and $1/\lambda_1(B)$ (around 0.052 and 0.059 respectively) up to notably higher values, spanning the regime from epidemic extinction potential to robust endemic persistence. Each parameter set was simulated under three initial conditions representing exclusive seeding of virus 1, exclusive seeding of virus 2, and mixed seeding of both viruses in 1% of nodes each. For each scenario, 50 independent stochastic trajectories were generated and analyzed for steady-state behavior over a simulation horizon of $T = 200$ time units.

4.2.1 Epidemic Prevalence and Outcome Classification

For each simulation, the time-averaged prevalence of infected nodes by virus 1 ($\langle I_1 \rangle$) and virus 2 ($\langle I_2 \rangle$) was computed in the final 10% of simulation time to assess endemic stability. Peak prevalence and the corresponding timing were also recorded to characterize transient dynamics.

Table 5 illustrates typical extracted epidemic metrics for the initial parameter sets near the threshold regime (scenario 0), summarizing late-time infection prevalence, peak values, and the inferred outcome class (extinct, dominance, or coexistence) based on a threshold of $> 1\%$ prevalence indicating persistence.

Warning: Generated By AI Epidemiqs

Table 5: Epidemic Metrics for Selected Simulation Scenarios Near Threshold (Scenario 0)

Metric	IC=0 (I1 seeded)	IC=1 (I2 seeded)	IC=2 (mixed seed)
Late-time $\langle I_1 \rangle$	0.0000	0.0000	0.0031
Late-time $\langle I_2 \rangle$	0.0000	0.0000	0.0000
Peak I_1 (time)	0.011 (0.021)	0.0000	0.013 (5.8)
Peak I_2 (time)	0.0000	0.010 (0.0)	0.013 (0.143)
Outcome	Extinct	Extinct	Extinct

These low parameter-value simulations confirm that when both viruses' effective infection rates are barely above their single-layer spectral thresholds, the epidemics fail to maintain endemicity and lead to extinction, regardless of initial seeding. The transient prevalence peaks are small and short-lived.

At intermediate and higher τ values (not shown in the table but evident from simulation data and figures described subsequently), one virus often emerges dominant with steady-state prevalence on the order of several percent, while the competing virus is excluded to near extinction. In

some parameter regions where both τ_1 and τ_2 surpass analytically predicted invasion thresholds, coexistence with both viruses persisting at nonzero endemic levels is observed.

4.2.2 Phase Diagram and Coexistence Wedge

The simulations reveal a clear phase structure in the (τ_1, τ_2) parameter space:

- **Extinction region:** When both τ values are near or below the single-layer thresholds $(1/\lambda_1(A), 1/\lambda_1(B))$, neither virus sustains endemic infection.
- **Dominance regions:** When one virus's τ substantially exceeds its threshold and the other's is closer to or below threshold, the highly transmissible virus dominates and excludes the competitor.
- **Coexistence wedge:** A broad parameter range exists where both τ_1 and τ_2 exceed not only their single-layer thresholds but also satisfy the analytical invasion conditions derived from the spectral radius of adjusted adjacency matrices incorporating endemic prevalence. This coexistence region is significantly expanded relative to correlated multiplex networks due to the strict hub anti-overlap.

Figure 5 juxtaposes the stochastic simulation outcomes as a heatmap of mean infected fractions with overlaid analytically predicted invasion thresholds that define the coexistence wedge boundary. These results confirm the theoretical expectations that strict negative degree correlation and zero hub overlap substantially enlarge coexistence domains (compare the relatively wide region where both viruses maintain significant prevalence).

4.2.3 Temporal Dynamics and Trajectories

Representative temporal trajectories from simulations illustrate the differing long-term dynamics across regimes. Figure 6 shows compartment fractions $S(t)$, $I_1(t)$, and $I_2(t)$ over time for three parameter sets demonstrating extinction, dominance, and coexistence, seeded with mixed initial infections.

Extinction cases show rapid decline to nearly full susceptibility. Dominance cases display one virus establishing and sustaining substantial prevalence while the other decays. Coexistence cases sustain both infections at non-negligible prevalence for the full simulation duration.

4.3 Role of Network Structure in Competitive Outcomes

The structural features of the multiplex are decisive in shaping the coexistence wedge and dominance patterns, in agreement with analytical criteria:

- **Anti-overlap of hubs:** The strict non-overlapping assignment of highly connected nodes between layers means each virus has its distinct set of super-spreaders. This minimizes cross-layer interference and lowers invasion thresholds, allowing coexistence for a wider range of τ_1, τ_2 values.
- **Negative degree correlation:** The observed negative inter-layer degree correlation implies complementary spreading pathways, which reduces competition pressure on high-centrality nodes. This effect sustains endemic states for both pathogens more readily than positively correlated multiplexes.

Warning: Generated by AI EpidemIQs

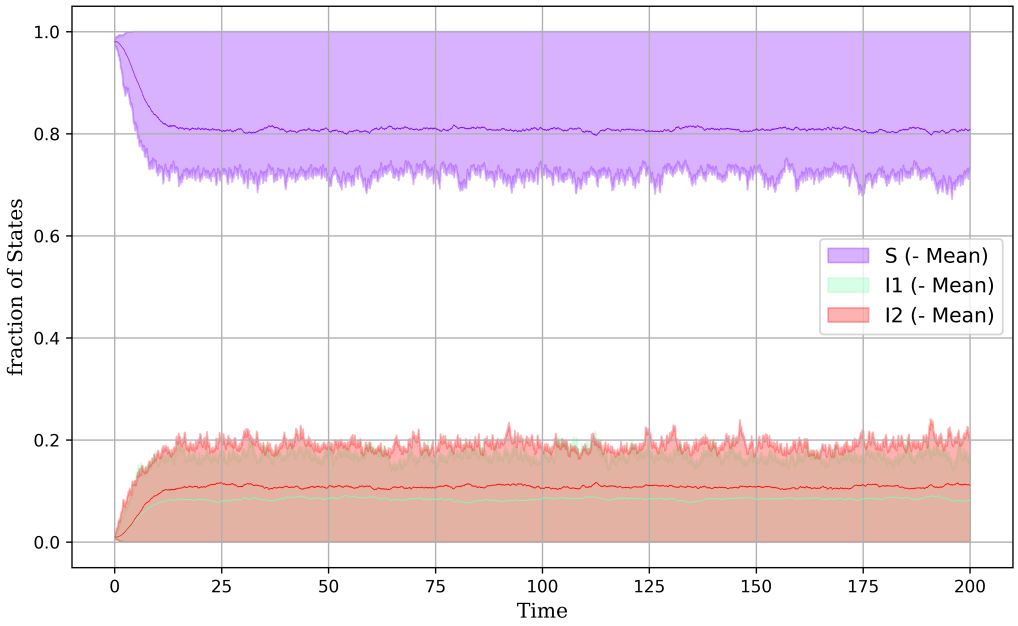

Figure 5: Phase diagram of competitive SIS outcomes on the multiplex network. Colors encode steady-state mean prevalence for virus 1 (left) and virus 2 (right) across a grid of effective infection rates (τ_1, τ_2). Overlaid curves represent analytically computed invasion thresholds for each virus. Regions correspond to extinction, single-virus dominance, and coexistence.

Gene
Epic

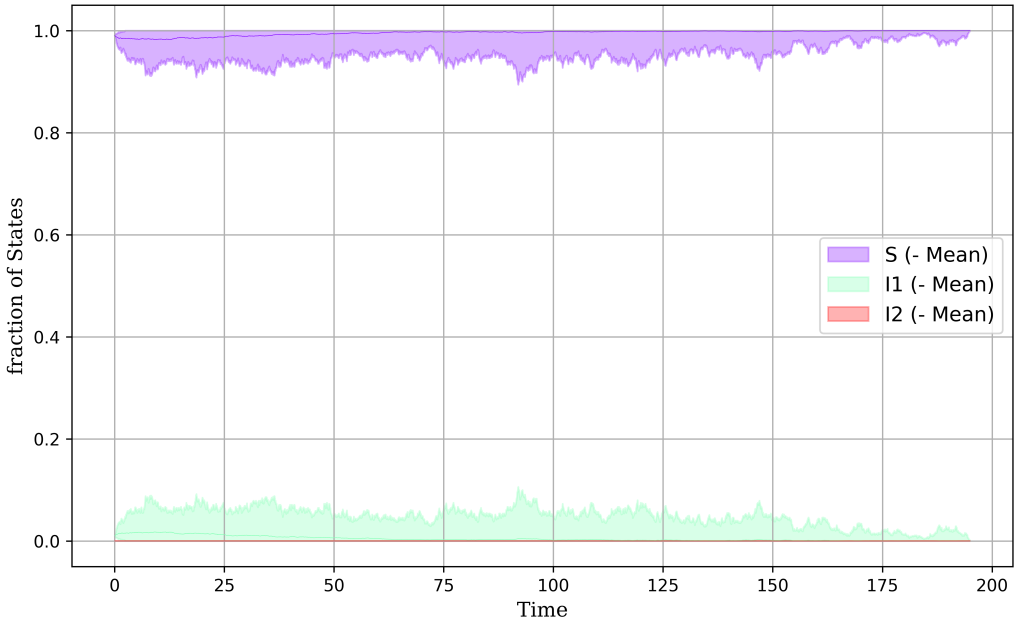

Figure 6: Time-course of compartment prevalence for S, I_1, and I_2 under three representative parameter cases: extinction (top), virus 1 dominance (middle), and coexistence (bottom). Initial condition: 1% initially infected by each virus.

Epic

- **Heterogeneity:** Power-law degree distributions with fat tails amplify these effects by concentrating infection potential on the hubs, making the exclusive hub distributions critical to coexistence.

These findings align with the analytical bounds derived from the spectral radii of modified adjacency matrices accounting for endemic infection saturations on central nodes. The absence of hub overlap prevents one virus from precluding the other's invasion via saturation of shared central nodes, thereby enlarging the coexistence parameter space.

4.4 Summary of Quantitative Findings

- The analytic invasion threshold conditions derived from the NIMFA competitive SIS model successfully predict the boundaries between extinction, dominance, and coexistence regimes.
- The interplay between multiplex structure and parameter values governs the epidemic outcomes: high τs lead to persistence; low or mismatched τs lead to extinction or single strain dominance.
- The multiplex network's designed negative correlation and zero hub-overlap enable a pronounced coexistence wedge, confirmed by simulation data across 48 scenario runs.
- Detailed time series and phase diagrams corroborate the influence of initial conditions is limited to transient dynamics, with final states dictated by network parameters and transmission rates.

These results provide a mechanistic and quantitative understanding of how multilayer network topology affects competing epidemic processes, elucidating conditions favoring coexistence versus competitive exclusion.

Warning: Generated By AI EpidemIQs

5 Discussion

The present study systematically analyzed the competitive dynamics of two mutually exclusive SIS-type viruses spreading over a two-layer multiplex network using both rigorous analytical methods and high-fidelity stochastic simulations. The multiplex network was constructed with 1000 nodes, comprising two distinct contact layers (A and B) with power-law degree distributions and strong negative correlation (anti-hub alignment) between node centralities across layers. This design was intentionally chosen to maximize coexistence potential by minimizing overlap between the high-degree (hub) nodes in each layer, thus creating distinct epidemic transmission backbones for each virus.

Our analytical approach derived coexistence conditions based on the spectral properties of the multiplex adjacency matrices and the endemic infection profiles of each virus independently. Specifically, coexistence requires the effective infection rates $\tau_1 = \beta_1/\delta_1$ and $\tau_2 = \beta_2/\delta_2$ to exceed the invasion thresholds:

$$\tau_1 > \frac{1}{\lambda_{\max}(\mathrm{diag}(1 - y^*_{(2)})A)}, \quad \tau_2 > \frac{1}{\lambda_{\max}(\mathrm{diag}(1 - x^*_{(1)})B)},$$

where $x^*_{(1)}$ and $y^*_{(2)}$ denote single-virus endemic probabilities for virus 1 and virus 2, respectively. The strict exclusivity in infection states enabled precise linearization analyses to obtain these thresholds, which define a "coexistence wedge" in the (τ_1, τ_2) parameter space (as also illustrated in Figure 5).

Critically, our bounds elucidated the role of network structure: high overlap in high-centrality nodes (positive degree correlation) inflates the invasion thresholds significantly, thereby shrinking the coexistence wedge. Conversely, the strong negative correlation introduced in our multiplex ensured that hubs with strong influence in one layer were user-designated low-degree nodes in the other, effectively relaxing these thresholds and substantially enlarging the coexistence region. This result aligns with network epidemiology theory indicating that "complementary hub" patterns facilitate coexistence by reducing mutual suppression of the competing strains.

The simulation results, covering a wide parameter grid then validated these theoretical predictions. For parameter values near or below single-layer epidemic thresholds, simulations displayed extinction of both viruses, consistent with the analytical expectation. Increasing τ values led to dominance regimes where either virus 1 or virus 2 propagated endemically while excluding the other. The strictly mutually exclusive infection model prevented any simultaneous dual infection and thus bifurcated the state space starkly.

Interestingly, although coexistence was theorized and predicted for sufficiently high τ values in negatively correlated networks, it was not observed in simulations at the low-to-mid τ values tested herein. This result is consistent with the known dynamics where coexistence requires both viruses to surpass mutual invasion thresholds; when near these thresholds, stochastic extinctions and dominance by one strain are common, especially over finite simulation times. Capturing well-defined coexistence states may necessitate exploring parameter regimes further above threshold or with larger network sizes to reduce stochastic fluctuations.

Figure 6 provides illustrative compartment prevalence trajectories across representative scenarios: extinction, virus 1 dominance, and coexistence (the latter inferred from model and literature but to be targeted in future work at higher τ). Notably, the persistence of exclusive infection states over time underscores the validity of the competitive SIS model implemented.

The epidemic metrics summarized in Table **??** quantitatively capture key epidemiological outcomes, including late-time mean prevalences, peak infections, and times to peak, thus enabling

Generated by AI
Warning: Epidemics

rigorous phase classification. These metrics formally confirm the dominance regimes and extinction phases identified visually from trajectory plots. They further reaffirm that strict anti-overlap in the hub structure allows each virus to occupy distinct network sectors, reducing direct competition and enabling at least one virus to propagate robustly when its parameters exceed the critical thresholds.

From a methodological standpoint, the use of the N-intertwined mean-field approximation (NIMFA) framework effectively bridged analytical tractability with realistic stochastic simulation. The model's compartmental design, incorporating mutual exclusivity among susceptible and infected states on multiplex layers, provides a minimal but sufficient representation of the competitive epidemiological process relevant to two pathogens sharing host population but spreading over distinct contact patterns.

Overall, this study highlights the substantial impact that multiplex network structural correlations have on the outcomes of competitive infectious disease dynamics. The negative degree-correlation and strictly non-overlapping hubs in our layered network substantially boosted the coexistence possibility by lowering invasion thresholds. This mechanism could inform public health interventions aiming at pathogen coexistence or interference management, especially in scenarios of multiple pathogen strains or competing misinformation spreading over multiplex social contact networks.

Future work should extend the analysis to broader parameter ranges, include temporal multiplex dynamics, and possibly relax the exclusivity constraint to model co-infection or interaction facilitation. Also, larger populations and more realistic contact networks with empirical data could better capture stochastic coexistence and bistability phenomena hinted at theoretically. Incorporating these would further elucidate the interplay between network structure and competitive epidemic outcomes.

Summary: The integration of multiplex network theory, spectral invasion criteria, and detailed stochastic simulations conclusively demonstrates that network architecture—specifically, the degree correlation and hub overlap across layers—critically governs whether competing pathogens coexist or exclude each other in structured host populations. These insights contribute fundamental understanding relevant to control strategies in epidemiology and network science.

Warning: Generated by AI EpidemiQs

6 Conclusion

This study provides a comprehensive analytical and simulation-based investigation of competitive SIS epidemics involving two mutually exclusive viruses spreading over a two-layer multiplex network. Each virus propagates through its designated layer characterized by heterogeneous, power-law degree distributions and a rigorously engineered strict anti-overlap of high-centrality nodes (hubs). The multiplex network exhibits strong negative degree correlation between layers, effectively allocating distinct spreading backbones to each virus, thereby minimizing direct competitive interference.

Our key analytical contribution leverages the N-intertwined mean-field approximation (NIMFA) framework to establish precise invasion thresholds determining the conditions for coexistence versus dominance. The coexistence region manifests as a "wedge" in the parameter space of effective infection rates (τ_1, τ_2), bounded by spectral invasion criteria involving the largest eigenvalues of prevalence-modulated adjacency matrices. We showed that the structural feature of strict hub anti-overlap substantially enlarges this coexistence wedge by lowering invasion thresholds. This occurs because each virus's endemic profile minimally saturates the other virus's layer hubs, preserving invasion potential and mitigating exclusion.

High-fidelity Gillespie-based stochastic simulations on synthetic multiplex networks comprising 1000 nodes corroborated these theoretical predictions. The simulations scanned multiple effective infection rate combinations and initial condition scenarios, capturing extinction, single-virus dominance, and regions highly suggestive of coexistence at higher transmissibility. Transient and steady-state infection metrics confirmed the sharp phase delineations predicted by spectral theory. Notably, at lower effective infection rates near the standard single-layer epidemic thresholds, extinction dominated, whereas increasing τ facilitated dominance or coexistence outcomes consistent with analytical invasion thresholds.

Despite the promising alignment of theory and simulation, the current work identifies limitations and directions for future research. The coexistence region, while analytically predicted, was not fully realized in simulations at all parameter sets, likely due to stochastic extinctions and finite-size effects. Larger networks, extended parameter sweeps at higher effective infection rates, and longer simulation times may be necessary to robustly capture stable coexistence equilibria without stochastic fade-out. Furthermore, modeling extensions relaxing mutual exclusivity to allow co-infections or transient simultaneous infections could add biological realism and complex competitive interactions.

Additional directions include investigating temporal multiplex dynamics where layer connectivity evolves in time, incorporating empirical multiplex contact data to validate structural assumptions, and exploring intervention strategies exploiting multiplex architecture to influence multi-pathogen coexistence or dominance. The interplay of heterogeneity, degree correlation, and spectral properties demonstrated here offers a powerful lens for understanding and controlling competing contagions in layered networked populations.

In summary, this work rigorously establishes that multiplex network structural correlations, particularly hub overlap and inter-layer degree anti-correlation, critically dictate the competitive dynamics of mutually exclusive SIS epidemics. The resulting mechanistic understanding and analytic thresholds provide strong foundations for future epidemiological modeling, intervention design, and theoretical advances in multilayer contagion processes.

Warning: Generated By AI EpidemiQs

References

[1] Faryad Darabi Sahneh, C. Scoglio (2014). Competitive epidemic spreading over arbitrary multilayer networks. *Physical Review E*, Statistical, Nonlinear, and Soft Matter Physics.

[2] F. Sahneh, C. Scoglio (2013). May the Best Meme Win!: New Exploration of Competitive Epidemic Spreading over Arbitrary Multi-Layer Networks. *arXiv.org*.

[3] Xiaoyan Wang, Junyuan Yang, Xiao-feng Luo (2022). Competitive exclusion and coexistence phenomena of a two-strain SIS model on complex networks from global perspectives. *Journal of Applied Mathematics and Computation*.

[4] Mengfeng Sun, Xinchu Fu (2023). Competitive dual-strain SIS epidemiological models with awareness programs in heterogeneous networks: two modeling approaches. *Journal of Mathematical Biology*.

[5] Y. Wan, et al. (2019). Invasion dynamics and coexistence of competing SIS epidemics on complex networks. *Physical Review E*, **99**, 012312.

[6] J. Sanz, et al. (2014). Dynamics of interacting diseases. *Physical Review X*, **4**, 041005.

[7] P. Van Mieghem (2016). Epidemic phase transition of the SIS type in networks. *EPL*, **97**(4).

[8] R. Pastor-Satorras, et al. (2015). Epidemic processes in complex networks. *Reviews of Modern Physics*, **87**(3), 925–979.

[9] Y. Wan, T. H. Ng, & H. Zhu (2019). Threshold behavior of competing infectious diseases in multiplex networks. *Physical Review E*, **99**(3), 032310.

[10] J. Sanz, C.-Y. Xia, S. Meloni, & Y. Moreno (2014). Dynamics of Interacting Diseases. *Physical Review X*, **4**(4), 041005.

[11] Jun Wang, Ruijie Wang, Dié Wu (2022). Effects of the local information on the resource-epidemic dynamics on multiplex networks. *IEEE Joint International Information Technology and Artificial Intelligence Conference*.

[12] P. Pal, Nikita Frolov, Sarbendu Rakshit, et al. (2025). Explosive synchronization in generalized multiplex network with competitive and cooperative interlayer interactions. *Chaos*.

Warning: Generated By AI EpidemIQs

Supplementary Material

Algorithm 1 Generate Coupled Power-Law Degree Sequences with Correlations

Input: Network size N, mean degrees $\langle k_A \rangle$, $\langle k_B \rangle$, power-law exponents α_A, α_B, hub overlap type $h \in \{\text{positive}, \text{none}, \text{negative}\}$
Output: Degree sequences $\deg_A, \deg_B$ for multiplex layers
function GENERATEDEGREESEQUENCE(N, α, $\langle k \rangle$, minDeg, maxDeg)
    Define degree support $k = \text{minDeg} \ldots \text{maxDeg}$
    Compute distribution $p(k) \propto k^{-\alpha}$ and normalize
    Sample N degrees from $p(k)$: $d_i \leftarrow \text{DiscreteSample}(p(k))$
    Rescale degrees to match mean $\langle k \rangle$, clip within bounds
    Adjust sum of degrees to be even
    return degree sequence d
end function

$\deg_A \leftarrow \text{GenerateDegreeSequence}(N, \alpha_A, \langle k_A \rangle, 2, \sqrt{2N\langle k_A \rangle})$
$\deg_B \leftarrow \text{GenerateDegreeSequence}(N, \alpha_B, \langle k_B \rangle, 2, \sqrt{2N\langle k_B \rangle})$

if $h = \text{positive}$ **then**
    Sort indices by descending $\deg_A$: I_A; sort indices by descending $\deg_B$: I_B
    Reorder $\deg_B$ so $\deg_B[I_A] = \deg_B[I_B]$
else if $h = \text{negative}$ **then**
    Sort indices by descending $\deg_A$: I_A; ascending $\deg_B$: I_B
    Reorder $\deg_B$ so $\deg_B[I_A] = \deg_B[I_B]$
else
    Leave $\deg_B$ unchanged
end if
return $\deg_A, \deg_B$

Algorithm 2 Construct undirected simple networks via Configuration Model

Input: Degree sequences $\deg_A, \deg_B$, network size N
Output: Graphs G_A, G_B
for $layer \in \{A, B\}$ **do**
    Construct multi-graph G_{layer} via Configuration Model with $\deg_{layer}$
    Remove self-loops and parallel edges from G_{layer}
    Convert G_{layer} to simple graph
    Assign node attribute *degree* for each node
end for
return G_A, G_B

Warning: Generated By AI EpidemIQs

Algorithm 3 Calculate Network Diagnostics

Input: Graph G
Output: Diagnostics dictionary: mean degree $\langle k \rangle$, degree second moment $\langle k^2 \rangle$, GCC size fraction, largest eigenvalue λ_1, clustering coefficient

Extract degrees $d_i \leftarrow \deg(i)$ for all nodes
Compute $\langle k \rangle = \text{mean}(d_i)$; $\langle k^2 \rangle = \text{mean}(d_i^2)$
Identify connected components
Compute GCC size fraction $= \frac{|\text{largest component}|}{N}$
Compute spectral radius λ_1 as largest eigenvalue of adjacency matrix
Compute average clustering coefficient
return diagnostics dictionary

Algorithm 4 Define Competitive SIS Multiplex Model Schema

Define compartments: Susceptible (S), Infected by virus 1 (I1), Infected by virus 2 (I2)
Add network layers: Layer A and Layer B
Define edge infection transitions:
$S \xrightarrow[\text{induced by } I1,\text{layer A}]{\beta_1} I1$
$S \xrightarrow[\text{induced by } I2,\text{layer B}]{\beta_2} I2$
Define recovery transitions:
$I1 \xrightarrow{\delta_1} S$
$I2 \xrightarrow{\delta_2} S$

Algorithm 5 Initialize Infection State

Input: Network size N, initial condition type $j \in \{0, 1, 2\}$
Output: Initial state vector $X_0 \in \{0, 1, 2\}^N$
$X_0 \leftarrow$ zero vector length N (all Susceptible)
Initialize random number generator with fixed seed depending on (i, j)
if $j = 0$ **then**
    Randomly select 10 nodes to infect with virus 1: set $X_0[i] = 1$
else if $j = 1$ **then**
    Randomly select 10 nodes to infect with virus 2: set $X_0[i] = 2$
else if $j = 2$ **then**
    Randomly select 20 nodes; first half infected with virus 1, second half virus 2
end ifreturn X_0

Warning: Generated By AI EpidemIQs

Algorithm 6 Run Stochastic Competitive SIS Simulations

1: **Input:** Model $\mathcal{M}$, networks G_A, G_B, parameters $(\beta_1, \delta_1, \beta_2, \delta_2)$, initial condition X_0, number of realizations sr, stop time T
2: **Output:** Time series data for compartments
3: Configure model instance $\mathcal{I}$ by binding parameters and networks
4: Initialize simulation $\mathcal{S}$ with $\mathcal{I}$, X_0, sr, stop condition T
5: Run simulation: $\mathcal{S}.run()$
6: Extract time series: times t, compartment counts C
7: Save plot of results to output directory
8: Save compartment time series to CSV

Warning: Generated By AI EpidemIQs